Bioorganic & Medicinal Chemistry Letters 25 (2015) 664–667

Contents lists available at ScienceDirect

Bioorganic & Medicinal Chemistry Letters

journal homepage: www.elsevier.com/locate/bmcl

A sensitive and specific Raman probe based on bisarylbutadiyne for live cell imaging of mitochondria

Hiroyuki Yamakoshi [a,b], Almar Palonpon [a,d], Kosuke Dodo [a,b,c], Jun Ando [a,b,c,d], Satoshi Kawata [d], Katsumasa Fujita [a,c,d], Mikiko Sodeoka [a,b,c,*]

[a] Sodeoka Live Cell Chemistry Project, ERATO, Japan Science and Technology Agency, 2-1 Hirosawa, Wako-shi, Saitama 351-0198, Japan
[b] Synthetic Organic Chemistry Laboratory, RIKEN, 2-1 Hirosawa, Wako-shi, Saitama 351-0198, Japan
[c] CREST, Japan Science and Technology Agency, 2-1 Hirosawa, Wako, Saitama 351-0198, Japan
[d] Department of Applied Physics, Osaka University, 2-1 Yamadaoka Suita, Osaka 565-0871, Japan

ARTICLE INFO

Article history:
Received 24 October 2014
Revised 26 November 2014
Accepted 28 November 2014
Available online 5 December 2014

Keywords:
Raman
Imaging
Mitochondria
Triphenylphosphonium
Live cell

ABSTRACT

We previously showed that bisarylbutadiyne (BADY), which has a conjugated diyne structure, exhibits an intense peak in the cellular Raman-silent region. Here, we synthesized a mitochondria-selective Raman probe by linking bisphenylbutadiyne with triphenylphosphonium, a well-known mitochondrial targeting moiety. This probe, named MitoBADY, has a Raman peak 27 times more intense than that of 5-ethynyl-2′-deoxyuridine. Raman microscopy using submicromolar extracellular probe concentrations successfully visualized mitochondria in living cells. A full Raman spectrum is acquired at each pixel of the scanned sample, and we showed that simultaneous Raman imaging of MitoBADY and endogenous cellular biomolecules can be achieved in a single scan. MitoBADY should be useful for the study of mitochondrial dynamics.

Mitochondria play a central role in cell maintenance, including energy supply, cell death, regulation of calcium signaling and cellular metabolism. They have been the target of a number of bioactive molecules, drug candidates and functionalized molecules designed to induce various biological effects.[1] The ability to image mitochondria in live cells is extremely useful for understanding mitochondrial dynamics and its association with various biological processes. Fluorescence methods employing mitochondrion-staining probes are well suited for this purpose because of their high sensitivity and specificity.[2]

On the other hand, Raman microscopy is available as a complementary imaging technique that does not require any label, but uses scattered light from vibrations of biomolecules. Spatially resolved Raman spectra obtained by Raman microscopy reflect the local biochemical composition of the cell, and thus offer more information than is available from fluorescence probes. Label-free imaging of mitochondrial distribution in cells has been demonstrated using confocal Raman microscopy combined with multivariate image construction methods.[3] Mitochondria have also been visualized in cells in a simpler way, without the need for multivariate analysis, by detecting the resonant Raman peaks of cytochrome c, an endogenous protein abundant in the mitochondrial membrane.[4] However, the distribution and concentration of cytochrome *c* vary with cell types and conditions, and therefore cytochrome *c* is not always a reliable probe for mitochondria. For instance, during apoptosis, cytochrome *c* is released into the cytosol from mitochondria.[5] In addition, the Raman intensity of cytochrome *c* peaks is dependent upon the redox state, which in turn depends strongly on the physiological state of the cell.[6] Other types of cytochromes, such as cytochrome *b*, which exhibits similar Raman peaks, might also contribute to the detected Raman signals.[7] Other intrinsic Raman signals from the cell could possibly be used, but this is problematic because of poor molecular selectivity owing to the marked overlap of Raman signals from a variety of endogenous molecules.

Instead of using intrinsic Raman signals to obtain imaging contrast, an alternative strategy is to use an exogenous Raman probe whose signal appears in the Raman-silent region of the cell (1800–2800 cm^{-1}). Efforts along this direction have led us to develop alkyne-tag Raman imaging (ATRI) for visualization of specific small molecules in live cells.[8] In this technique, we tag molecules with an alkyne moiety whose vibrational frequency lies in the silent region of the cell, free from the interfering signals of endogenous molecules, and which is small enough to minimally perturb the behavior of the target small molecule.[9] We also investigated the structure-Raman shift/intensity relationships of alkynes

* Corresponding author. Tel.: +81 48 467 9373; fax: +81 48 462 4666.
E-mail address: sodeoka@riken.jp (M. Sodeoka).

http://dx.doi.org/10.1016/j.bmcl.2014.11.080
0960-894X/

and demonstrated that simultaneous imaging of two small molecules having different Raman shifts was possible. Among the different alkynyl structures that we tested, bisarylbutadiynes (BADY; Fig. 1a) showed the strongest Raman intensity, producing alkyne peaks about 25 times stronger than that of 5-ethynyl-2′-deoxyuridine (EdU) on average.[8b] Although BADY is a bulky Raman tag for visualization of small molecules, we expected that it could be used as a sensitive and specific Raman probe for visualizing cellular organelles such as mitochondria after addition of an appropriate targeting moiety. Here, we describe the synthesis of a mitochondrion-targeting Raman probe based on BADY (MitoBADY; Fig. 1b) and we demonstrate its utility for imaging mitochondria in live cells.

As a mitochondrial targeting moiety, we selected triphenylphosphonium, a liphophilic cation, that is accumulated in the negatively charged mitochondrial matrix.[10] It has been widely used to target anti-oxidants,[11] fluorogenic sensors,[12] photoactivated delivery systems[13] and other molecules[14] to mitochondria.

MitoBADY was easily synthesized from commercially available 4-ethynylbenzaldehyde (Scheme 1). The bisarylbutadiyne structure was constructed by means of Ni-catalyzed yne–yne coupling.[15] After reduction of the aldehyde, the benzylic alcohol was converted to triphenylphosphonium in two steps. In the Raman spectrum of the synthesized MitoBADY, the alkyne peak at 2218 cm^{-1} showed a relative Raman intensity vs EdU (RIE) of 27, in agreement with our previous report.[8b] The negligible fluorescence background in the Raman spectrum and the observed UV–vis absorption spectrum confirmed that MitoBADY is nonfluorescent upon visible light excitation.[16]

To investigate the potential of MitoBADY for live-cell imaging of mitochondria, HeLa cells were treated with 400 nM MitoBADY, and Raman images were acquired using a home-built slit-scanning Raman microscope.[17] At this concentration of MitoBADY, no precipitation was observed during the cellular experiments. Figure 2a shows the distributions of cytochrome *c* and MitoBADY, observed at 751 cm^{-1} and 2220 cm^{-1}, respectively, at various incubation times. The contrast of MitoBADY was observable within 5 min, indicating rapid uptake by the cells, and reached a steady state in 30 min, remaining relatively stable for at least 75 min.[18] The MitoBADY distribution coincided well with that of cytochrome *c* distribution in the colocalization images. The time-dependent uptake of MitoBADY was further supported by the relative intensities of the cytochrome *c* and MitoBADY peaks in the Raman spectra obtained from the cytosol (Fig. 2b). Since the cells in this experiment are non-apoptotic, the distribution of mitochondria is expected to be the same as that of cytochrome *c*, as was verified in subsequent experiments (see Fig. 3). Thus, our results show that MitoBADY selectively targets and accumulates in mitochondria.

The mitochondrial localization of MitoBADY in live cells was further confirmed by comparing the distribution of MitoBADY with that of a typical mitochondrion probe, MitoTracker Green FM (MTG). Live HeLa cells treated with and without 200 nM MitoBADY were stained with MTG for 10 min. The cells were then subjected to successive fluorescence and Raman imaging using the same slit-scanning microscope setup. These images coincided well, confirming

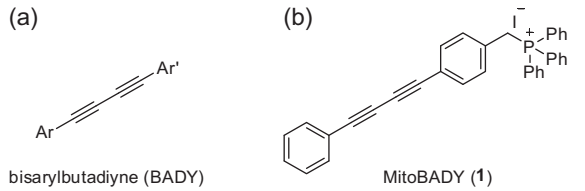

Figure 1. Structures of bisarylbutadiyne (BADY) and MitoBADY.

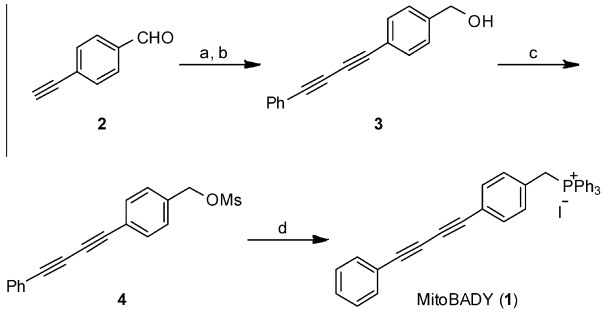

Scheme 1. Synthesis of MitoBADY. Reagents and conditions: (a) Ethynylbenzene, CuI, $NiCl_2{\cdot}6H_2O$, tetramethylethylenediamine, air, THF; (b) $LiAlH_4$, THF, 0 °C, 52% for 2 steps; (c) MsCl, Et_3N, CH_2Cl_2, 76%, (d) PPh_3, NaI, MeCN, 75 °C, 95%.

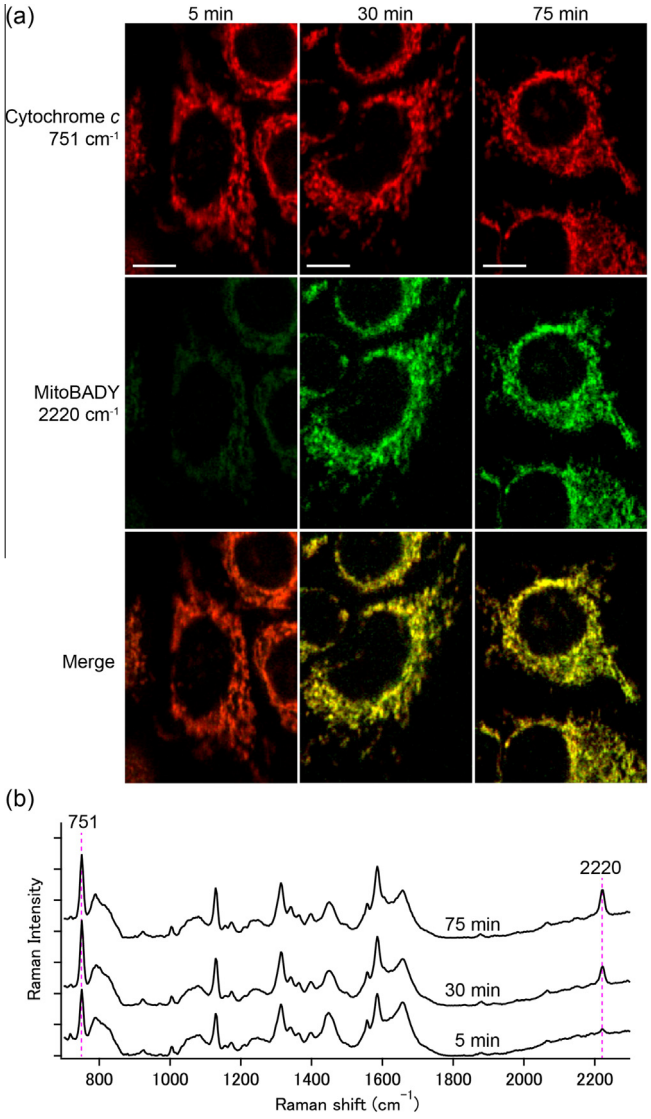

Figure 2. Raman imaging of MitoBADY in living cells. (a) Raman images showing the distributions of cytochrome *c* at 751 cm^{-1} (red) and MitoBADY at 2220 cm^{-1} (green) in live HeLa cells treated with 400 nM MitoBADY. Areas of colocalization in the merged image appear yellow. (b) Average Raman spectra obtained from the cytosol showing relative intensities of cytochrome *c* and MitoBADY peaks. Imaging conditions: laser wavelength, 532 nm; laser intensity, 3.3 mW/μm^2; exposure time, 5 s/line. Scale bar is 10 μm.

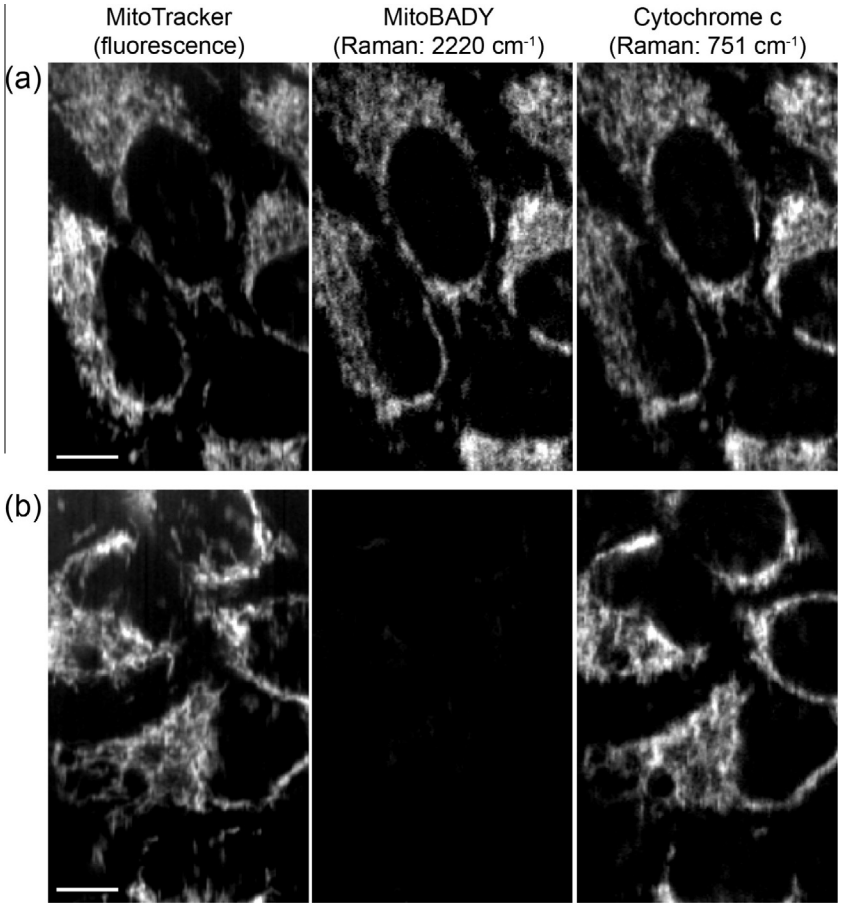

Figure 3. Sequential imaging of MTG and MitoBADY in living cells. Fluorescence and Raman images of HeLa cells treated with (a) 50 nM MTG and 200 nM MitoBADY and (b) 50 nM MTG only. The fluorescence imaging was done first, followed by Raman imaging. Imaging conditions: laser wavelength, 532 nm; laser intensity, 0.05 mW/μm^2 (fluorescence), 3.3 mW/μm^2 (Raman); exposure time, 0.2 s/line (fluorescence), 5 s/line (Raman); Scale bar is 10 μm.

the selective staining capability of MitoBADY for mitochondria (Fig. 3). In addition, the Raman image of cytochrome *c* shows the same distribution as that of MTG, establishing cytochrome *c* as another good Raman probe for mitochondria in the case of non-apoptotic cells under resonance excitation conditions. Note that the high laser intensity used in Raman imaging causes photobleaching of the MTG fluorophores so that no fluorescence from MTG is detected during Raman imaging; otherwise, this might interfere with the measurement of the Raman signals.

Since a full Raman spectrum is acquired at each pixel of the scanned sample, simultaneous Raman imaging of MitoBADY and endogenous cellular biomolecules is readily available from a single scan. As shown in Figure 4, the subcellular pattern of MitoBADY, which represents the distribution of mitochondria, is quite distinct from the patterns of endogenous protein and lipid, as identified from the amide-I (1686 cm^{-1}) and CH_2 stretching (2853 cm^{-1}) vibrations, respectively. This result demonstrates that organelle-specific Raman probes such as MitoBADY can be used to image specific cellular targets simultaneously with intrinsic biomolecules, thereby providing a great deal of chemical information about the cell.

In summary, we have synthesized and characterized a novel mitochondrion-targeting Raman probe called MitoBADY and applied it to cellular imaging of mitochondria. The bisphenyl-substituted diyne structure provides a Raman signal intensity 27 times higher than that of EdU, enabling application of the probe at submicromolar extracellular concentrations. Since the signal of MitoBADY appears in the Raman-silent region of the cell, it is possible

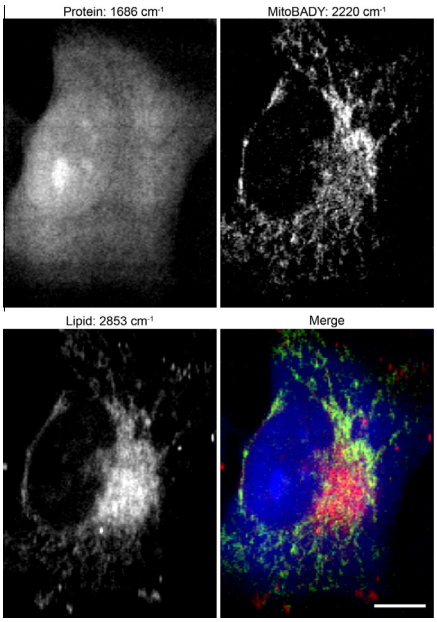

Figure 4. Simultaneous Raman imaging of MitoBADY and endogenous biomolecules in living cells. Raman images show the subcellular distributions of protein, MitoBADY, and lipid in live HeLa cells treated with 200 nM MitoBADY. Color channels in the merged image: blue, protein; green, MitoBADY; red, lipid. Imaging conditions: laser wavelength, 532 nm; laser intensity, 2.3 mW/μm^2; exposure time, 5 s/line; Scale bar is 10 μm.

to obtain Raman signals simultaneously from other endogenous compounds or exogenous molecules in the cell, making it possible to visualize the relationship of cellular components to cellular structures. It should be straightforward to develop Raman probes targeting other organelles by using BADY coupled with other targeting moieties, and this would extend the scope of Raman microscopy to the molecular analysis of specific cellular domains.

Acknowledgments

The authors thank Dr. Masaya Okada for technical support and helpful discussions. This work was partly supported by a Grant-in-Aid for Young Scientist (B) (23710276 to H.Y. and 2410267 to J.A.) from the Ministry of Education, Culture, Sports, Science, and Technology, Japan.

Supplementary data

Supplementary data (detailed description of the slit-scanning confocal Raman microscope, experimental procedures and characterization of all compounds) associated with this article can be found, in the online version, at http://dx.doi.org/10.1016/j.bmcl.2014.11.080.

References and notes

1. (a) Fulda, S.; Galluzi, L.; Kroemer, G. *Nat. Rev. Drug Discovery* **2010**, *9*, 447; (b) Szewczyk, A.; Wojtczak, L. *Pharmcol. Rev.* **2002**, *54*, 101.
2. (a) Zhang, J.; Campbell, R. E.; Ting, A. Y.; Tsien, R. Y. *Nat. Rev. Mol. Cell Biol.* **2002**, *3*, 906; (b) Neto, B. A. D.; Correa, J. R.; Silva, R. G. *RSC Adv.* **2013**, *3*, 5291.
3. (a) Matthäus, C.; Chernenko, T.; Newmark, J. A.; Warner, C. M.; Diem, M. *Biophys. J.* **2007**, *93*, 668; (b) Klein, K.; Gigler, A. M.; Aschenbrenner, T.; Monetti, R.; Bunk, W.; Jamitzky, F.; Morfill, G.; Start, R. W.; Schlegel, J. *Biophys. J.* **2012**, *102*, 360.
4. (a) Hamada, K.; Fujita, K.; Smith, N. I.; Kobayashi, M.; Inoue, Y.; Kawata, S. *J. Biomed. Opt.* **2008**, *13*, 044027; (b) Spiro, T. G.; Strekas, T. C. *Proc. Natl. Acad. Sci. U.S.A.* **1972**, *69*, 2622.
5. Okada, M.; Smith, N. I.; Palonpon, A. F.; Endo, H.; Kawata, S.; Sodeoka, M.; Fujita, K. *Proc. Natl. Acad. Sci. U.S.A.* **2012**, *109*, 28.
6. (a) Kakita, M.; Kaliaperumal, V.; Hamaguchi, H. *J. Biophotonics* **2012**, *5*, 20; (b) Kakita, M.; Okuno, M.; Hamaguchi, H. *J. Biophotonics* **2013**, *6*, 256.
7. Berezhna, S.; Wohlrab, H.; Champion, P. M. *Biochemistry* **2003**, *42*, 6149.
8. (a) Yamakoshi, H.; Dodo, K.; Okada, M.; Ando, J.; Palonpon, A.; Fujita, K.; Kawata, S.; Sodeoka, M. *J. Am. Chem. Soc.* **2011**, *133*, 6102; (b) Yamakoshi, H.; Dodo, K.; Palonpon, A.; Ando, J.; Fujita, K.; Kawata, S.; Sodeoka, M. *J. Am. Chem. Soc.* **2012**, *134*, 20681.
9. Alkyne-tag Raman imaging is fast becoming a general strategy for detection of specific molecules coupled with other detection systems. Recent examples with stimulated Raman scattering (SRS) microscopy, see: (a) Hong, S.; Chen, T.; Zhu, Y.; Li, A.; Huang, Y.; Chen, X. *Angew. Chem., Int. Ed.* **2014**, *53*, 5827; (b) Chen, Z.; Paley, D. W.; Wei, L.; Weisman, A. L.; Friesner, R. A.; Nuckolls, C.; Min, W. *J. Am. Chem. Soc.* **2014**, *136*, 8027; (c) Wei, L.; Hu, F.; Shen, Y.; Chen, Z.; Yu, Y.; Lin, C.-C.; Wang, M. C.; Min, W. *Nat. Methods* **2014**, *11*, 410.
10. (a) Liberman, E. A.; Topaly, V. P.; Tsofina, L. M.; Jasaitis, A. A.; Skulachev, V. P. *Nature* **1969**, *222*, 1076; (b) Grinius, L. L.; Jasatis, A. A.; Kadziauskas, Y. P.; Liberman, E. A.; Skulachev, V. P.; Topali, V. P.; Tsofina, L. M.; Vladimirova, M. A. *Biochim. Biophys. Acta* **1970**, *216*, 1.
11. Kelso, G. F.; Porteous, C. M.; Coulter, C. V.; Hughes, G.; Porteous, W. K.; Ledgerwood, E. C.; Smith, R. A. J.; Murphy, M. P. *J. Biol. Chem.* **2001**, *276*, 4588.
12. Selected recent examples of fluorogenic sensors, see: (a) Bae, S. K.; Heo, C. H.; Choi, D. J.; Sen, D.; Joe, E.-H.; Cho, B. R.; Kim, H. M. *J. Am. Chem. Soc.* **2013**, *135*, 9915; (b) Krumova, K.; Greene, L. E.; Cosa, G. *J. Am. Chem. Soc.* **2013**, *135*, 17135; (c) Hou, J.-T.; Wu, M.-Y.; Li, K.; Yang, J.; Yu, K.-K.; Xie, Y.-M.; Yu, X.-Q. *Chem. Commun.* **2014**, 8640.
13. Horinouchi, T.; Nakagawa, H.; Suzuki, T.; Fukuhara, K.; Miyata, N. *Bioorg. Med. Chem. Lett.* **2011**, *21*, 2000.
14. Selected examples of bioactive molecules, molecular probes, donors, and modulators, see: (a) Srivastava, P. C.; Kmapp, F. F., Jr. *J. Med. Chem.* **1984**, *27*, 978; (b) Burns, R. J.; Smith, R. A. J.; Murphy, M. P. *Arch. Biochim. Biophys.* **1995**, *322*, 60; (c) Hardy, M.; Chalier, F.; Ouari, O.; Finet, J.-P.; Rockenbauer, A.; Kalyanaraman, B.; Tordo, P. *Chem. Commun.* **2007**, 1083; (d) Ban, S.; Nakagawa, H.; Suzuki, T.; Miyata, N. *Bioorg. Med. Chem. Lett.* **2007**, *17*, 2055; (e) Biasutto, L.; Mattarei, A.; Marotta, E.; Bradaschia, A.; Sassi, N. *Bioorg. Med. Chem. Lett.* **2008**, *18*, 5594; (f) Prime, T. A.; Blaikie, F. H.; Evans, C.; Nadtochiy, S. M.; James, A. M.; Dahm, C. C.; Vitturi, D. A.; Patel, R. P.; Hiley, C. R.; Abakumova, I.; Requejo, R.; Chouchani, E. T.; Hurd, T. R.; Garvey, J. F.; Taylor, C. T.; Brookes, P. S.; Smith, R. A. J.; Murphy, M. P. *Proc. Natl. Acad. Sci. U.S.A.* **2009**, *106*, 10764; (g) Malouitre, S.; Dube, H.; Selwood, D.; Crompton, M. *Biochem. J.* **2010**, *425*, 137; (h) Atkinson, J.; Kapralov, A. A.; Yanamala, N.; Tyurina, Y. Y.; Amoscato, A. A.; Pearce, L.; Peterson, J.; Huang, Z.; Jiang, J.; Samhan-Arias, A. K.; Maeda, A.; Feng, W.; Wasserloos, K.; Belikova, N. A.; Tyurin, V. A.; Wang, H.; Fletcher, J.; Wang, Y.; Vlasova, I. I.; Klein-Seetharaman, J.; Stoyanovsky, D. A.; Bayîr, H.; Pitt, B. R.; Epperly, M. W.; Greenberger, J. S.; Kagan, V. E. *Nat. Commun.* **2011**, *2*, 497; (i) Cochemé, H. M.; Quin, C.; McQuaker, S. J.; Cabreiro, F.; Logan, A.; Prime, T. A.; Abakumova, I.; Patel, J. V.; Fearnley, I. M.; James, A. M.; Porteous, C. M.; Smith, R. A. J.; Saeed, S.; Carré, J. E.; Singer, M.; Gems, D.; Hartley, R. C.; Partridge, L.; Murphy, M. P. *Cell Metab.* **2011**, *13*, 340; (j) Masanta, G.; Lim, C. S.; Kim, H. J.; Han, J. H.; Kim, H. M.; Cho, B. R. *J. Am. Chem. Soc.* **2011**, *133*, 5698; (k) Tyurina, Y. Y.; Tungekar, M. A.; Jung, M.-Y.; Tyurin, V. A.; Greenberger, J. S.; Stoyanovsky, D. A.; Kagan, V. E. *FEBS Lett.* **2012**, *586*, 235; (l) Kelso, G. F.; Maroz, A.; Cochemé, H. M.; Logan, A.; Prime, T. A.; Peskin, A. V.; Winterbourn, C. C.; James, A. M.; Ross, M. F.; Brooker, S.; Porteous, C. M.; Anderson, R. F.; Murphy, M. P.; Smith, R. A. J. *Chem. Biol.* **2012**, *19*, 1237; (m) Murase, T.; Yoshihara, T.; Tobita, S. *Chem. Lett.* **2012**, *41*, 262; (n) Yang, Z.; He, Y.; Lee, J.-H.; Park, N.; Suh, M.; Chae, W.-S.; Cao, J.; Peng, X.; Jung, H.; Kang, C.; Kim, J.-S. *J. Am. Chem. Soc.* **2013**, *135*, 9181; (o) Constant-Urban, C.; Charif, M.; Goffin, E.; Van Heugen, J.-C.; Elmoualiji, B.; Chiap, P.; Mouithys-Mickalad, A.; Serteyn, D.; Lebrun, P.; Pirotte, B.; Tullio, P. D. *Bioorg. Med. Chem. Lett.* **2013**, *23*, 5878; (p) Leung, C. W. T.; Hong, Y.; Chen, S.; Zhao, E.; Lam, J. W. Y.; Tang, B. Z. *J. Am. Chem. Soc.* **2013**, *135*, 62; (q) Pathak, R. K.; Marrache, S.; Harn, D. A.; Dhar, S. *ACS Chem. Biol.* **2014**, *9*, 1178; (r) Trionnaire, S. L.; Perry, A.; Szczesny, B.; Szabo, C.; Winyard, P. G.; Whatmore, J. L.; Wood, M. E.; Whiteman, M. *Med. Chem. Commun.* **2014**, *5*, 728.
15. Yin, W.; He, C.; Chen, M.; Zhang, H.; Lei, A. *Org. Lett.* **2009**, *11*, 709.
16. Raman and UV–vis absorption spectrum of MitoBADY: See Supplementary data.
17. (a) Palonpon, A. F.; Ando, J.; Yamakoshi, H.; Dodo, K.; Sodeoka, M.; Kawata, S.; Fujita, K. *Nat. Protoc.* **2013**, *8*, 677; (b) Palonpon, A. F.; Sodeoka, M.; Fujita, K. *Curr. Opin. Chem. Biol.* **2013**, *17*, 708.
18. Ross, M. F.; Prime, T. A.; Abakumova, I.; James, A. M.; Porteous, C. M.; Smith, R. A.; Murphy, M. P. *Biochem. J.* **2008**, *411*, 633.